06.1;06.5

Creep in wood studied via continuous nanoindentation ranging from nano- to macro-scale

© Yu.I. Golovin[1,2], A.A. Gusev[1,3,4], A.I. Tyurin[1], D.Yu. Golovin[1], I.A. Vasyukova[1], M.A. Yunack[1]

[1] Tambov State University, Tambov, Russia
[2] Department of Chemistry, Moscow State University, Moscow, Russia
[3] Voronezh State University of Forestry and Technologies named after G.F. Morozov, Voronezh, Russia
[4] National University of Science and Technology MISiS, Moscow, Russia
E-mail: yugolovin@yandex.ru

Received November 7, 2022
Revised December 2, 2022
Accepted December 2, 2022

The paper presents the results of creep measurement in common pine wood at different scales ranging from nano to macro by means of continuous nanoindentation. It is shown that wood structure elements pertaining to different scale levels make different contribution to steady creep rate.

Keywords: nanoindentation, wood, creep.

DOI: 10.21883/TPL.2023.02.55365.19417

The trend toward construction of environmentally responsible residential and public buildings and application of renewable materials and green technology reinvigorated the interest in wood and other cellulose-based products as widely available natural constructional and structural materials [1–3]. Quite a few mechanical parameters of various types of wood have been studied fairly thoroughly in compression, tension, bending, torsion, hardness, shear, etc., tests [1,4]. Their dependences on porosity and density were determined, and the influence of the chemical composition, temperature, and humidity was established [5,6]. A considerable number of papers focused on the influence of creep on rigidity, strength, and reliability of woodwork [7,8] and on the influence of applied stress, humidity, and temperature on creep parameters [9–11] have already been published. However, the nature of creep at nano- and microlevels and the contribution of different structural components to long-term macromechanical properties of wood remain understudied.

The aim of the present study is to examine creep patterns in one of the most widely used types of wood (common pine wood, *Pinus sylvestris L.*) at different scales and hierarchical levels (from nano- to macroscale). The contribution of individual structural components to macromechanical time-dependent properties of wood was revealed by continuous nanoindentation (NI) [12–14]. The NI method has the following useful feature: the size and volume of the plastic deformation zone below a pyramidal indenter may increase by several orders of magnitude as it penetrates deeper into the tested material. This provides an opportunity to probe structural elements of various scales in deformation tests performed using one and the same measurement technique and the same sample and examine the associated size effects varying maximum load P_{max} applied to an indenter [15–20].

In the present study, we investigate the creep of early (EW) and late (LW) common pine wood in an annual growth ring corresponding to the year 2007 by NI of a transverse trunk section. Early wood forms at the beginning of growth of a ring and is characterized by low density and strength values, while late wood forms at the end stage,

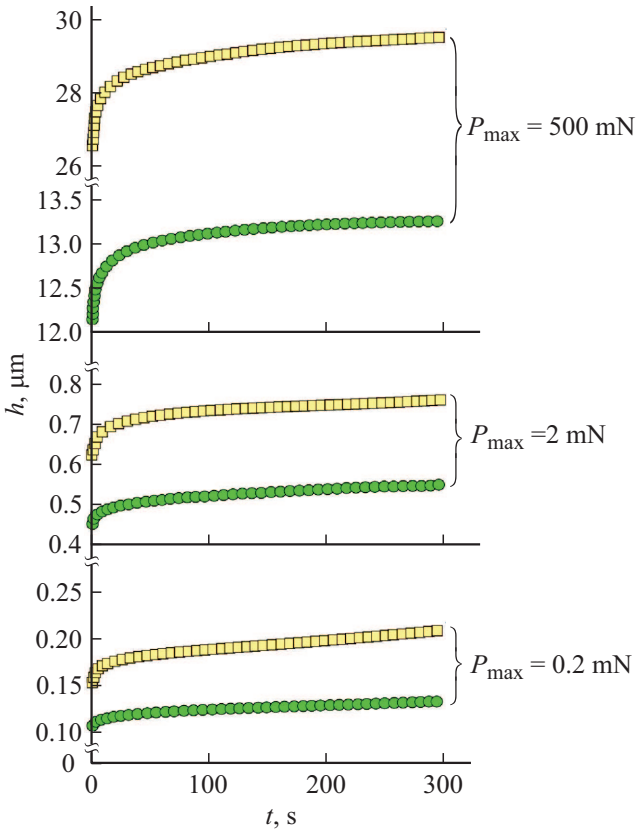

Figure 1. Creep kinetics under nanoindentation of early (squares) and late (circles) pine wood cells at different P_{max} values.

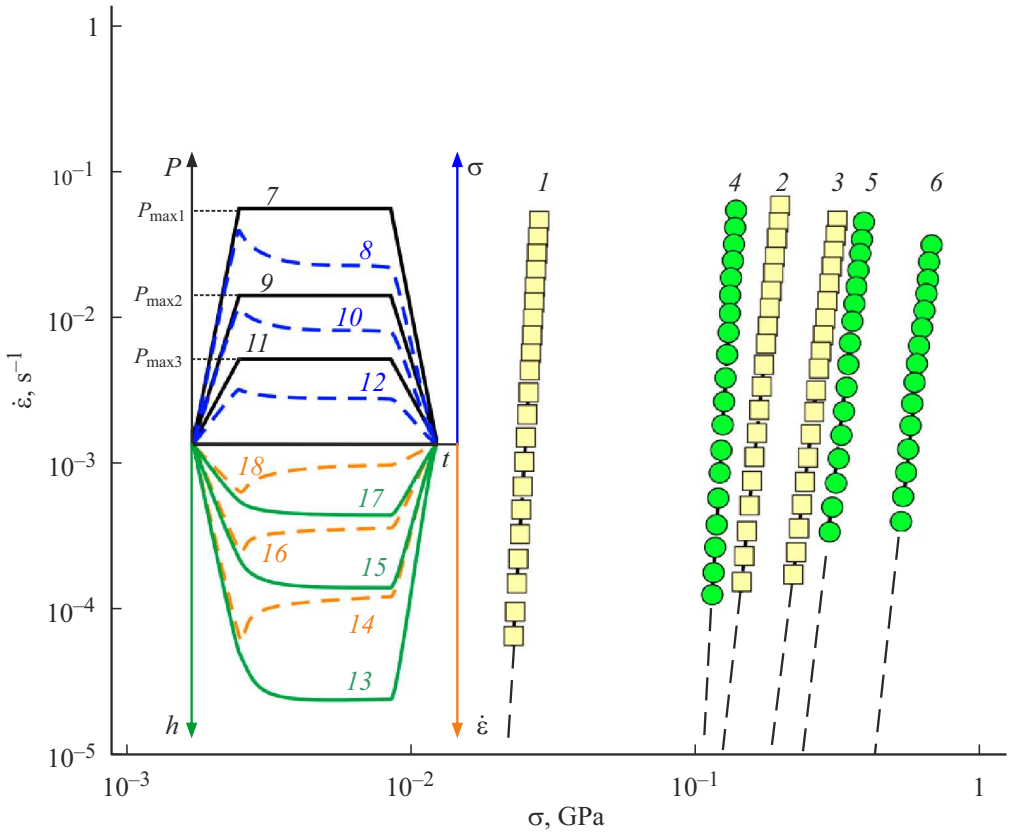

Figure 2. Dependence of steady-state creep rate $\dot{\varepsilon}$ on contact stress σ under nanoindentation of early (squares) and late (circles) pine wood cells. *1* — EW ($P_{max} = 500\,mN$), *2* — EW ($P_{max} = 2\,mN$), *3* — EW ($P_{max} = 0.2\,mN$), *4* — LW ($P_{max} = 500\,mN$), *5* — LW ($P_{max} = 2\,mN$), *6* — LW ($P_{max} = 0.2\,mN$). Kinetic dependences $P(t)$ (*7, 9, 11*), $\sigma(t)$ (*8, 10, 12*), $h(t)$ (*13, 15, 17*), and $\dot{\varepsilon}(t)$ (*14, 16, 18*) at different values of P_{max} ($P_{max\,1}$, $P_{max\,2}$, and $P_{max\,3}$) are shown schematically in the inset.

is denser, and features better mechanical characteristics. Samples were taken from a saw cut of a 110-year-old tree that grew in the Vernadskoe forest district of the Tambov Oblast.

A Hysitron TI-950 (USA) nanoindentometer fitted with a sharp 3-sided pyramidal diamond Berkovich indenter with a curvature radius at the tip of approximately 30 nm was used to examine the creep of selected wood samples. A nanoindentometer is a precision nano-micromechanical test machine that records a load–unload diagram as an indenter penetrates into a sample. The resolution is $\sim 50\,nN$ in force P and $\sim 0.5\,nm$ in depth h of indentation. The software bundled with the instrument allows one to program the needed time profile of force $P(t)$ and record dependence $h(t)$. A computer-controlled three-axis stage provides an opportunity to map mechanical properties over a large number of points (up to 10^3). Coordinates of points on the sample surface are entered into the test log, and further testing is performed without the intervention of an operator. A trapezoidal force $P(t)$ profile was used. Following a 30 s growth stage, the indenter load was maintained at a constant level within an interval of P_{max} from 0.2 to 500 mN by feedback circuits of the instrument. At the onset of loading, the point of indentation was aligned with a cell wall in all experiments.

Figure 1 presents the creep kinetics for different values of P_{max}. Loading stages and the behavior of measured quantities are shown schematically in the inset of Fig. 2. These data were obtained by averaging the results of 5-10 independent experiments. It follows from Fig. 1 that absolute deformation $h(t)$ under creep conditions increases with P_{max}, while the deformation rate decreases with time. At equal loads, creep is more pronounced in early wood. This is in line with the differences in other mechanical properties of EW and LW (specifically, the lower hardness of EW [18,19]).

Knowing the actual creep kinetics at the $P_{max} = const$ stage and the geometry of the penetrating indenter, one may determine steady-state creep rates $\dot{\varepsilon} = dh/(hdt)$ and average contact stress $\sigma = P_{max}A^{-1}$ below the indenter (A is the current indent area). The data presented in log-log coordinates $\lg\dot{\varepsilon} = f(\lg\sigma)$ (Fig. 2) demonstrate that the force dependence at the steady-state creep stage follows a power law: $\dot{\varepsilon} = C + b\sigma^n$. The values of power exponent n at various loads and indent sizes are presented in the table. The chosen P_{max} range allowed us to probe structural components of wood at different scale

Values of power exponent n in the expression for steady-state creep and R-squared values (R^2) at various levels of maximum force P_{max} applied to the indenter

Maximum force P_{max}, applied to the indenter, mN	Wood type					
	Early wood (EW)			Late wood (LW)		
	Indent side a, μm	n	R^2	Indent side a, μm	n	R^2
0.2	1.6 ± 0.1	15.6	0.617	1.0 ± 0.1	16.9	0.789
0.5	2.4 ± 0.1	18.1	0.610	1.7 ± 0.1	17.1	0.898
2	5.7 ± 0.5	18.2	0.874	4.1 ± 0.6	17.4	0.865
30	42 ± 3	21.2	0.857	21 ± 3	22.3	0.857
100	94 ± 4	27.4	0.918	39 ± 4	30.3	0.936
500	220 ± 3	31.7	0.922	99 ± 7	34.6	0.968

levels: from several tens of nanometers to several hundred micrometers. At $P_{max} = 0.2$ mN, the local plastic deformation zone ($\sim 1\,\mu$m) below the indenter is significantly smaller than the cell wall thickness ($3-5\,\mu$m for EW and around $10\,\mu$m for LW). Therefore, the intrinsic mechanical properties of its material are measured in this case without the effect of free boundaries. In contrast, an indent at $P_{max} = 500$ mN covered $5-10$ cells with a crosswise size of $30-40\,\mu$m. The buckling failure and flexural deformation of cell walls, which exert a considerable negative influence on mechanical parameters and contribute to an increase in n, are important factors of mechanical behavior in this case. At $P_{max} = 2$ mN, an indent covers a single cell. When the indenter penetrates deeper into the material, it interacts with different components of the cell structure and capillary architecture, thus yielding intermediate values of mechanical characteristics and n. As for creep mechanisms in wood, the following may be surmised. Since cellulose nanofibers, which form the load-bearing frame of cell walls in any wood, have excellent mechanical characteristics (a Young's modulus of $150-180$ GPa and a breaking strength of $5-10$ GPa), viscoelastic slip of cellulose nano- and microfibers, which are bound to each other by relatively weak molecular forces, may be the primary creep mechanism.

Thus, it was demonstrated that automated scanning NI may complement efficiently and enhance the capabilities of traditional macroscopic methods for examination of creep of wood. The determined patterns of creep of common pine wood observed at different scales and hierarchical levels (from nano- to macroscale) allow one to estimate the contribution of individual structural components to macromechanical time-dependent properties of wood. It was found that the creep rate in EW is considerably higher than the one in LW. The creep rate increases as the local plastic deformation zone grows in size from a submicrometer level, which represents the material of cell walls, to submillimeter scales, which correspond to deformation of the entire architecture of the multicellular structure together with capillaries and bring NI closer to macrotests. This implies that the wood creep rate may be reduced effectively by establishing such cultivation conditions that facilitate an increase in thickness of cell walls, which should then occupy a larger fraction of the cross section.

Funding

This study was supported by the Russian Science Foundation (grant 21-14-00233). Equipment provided by the common use center of the Derzhavin Tambov State University, which is supported in part by the Ministry of Science and Higher Education of the Russian Federation under contract No. 075-15-2021-709 (unique project identifier RF-2296.61321X0037), was used to perform the experiments discussed above.

Conflict of interest

The authors declare that they have no conflict of interest.

References

[1] K.K. Pandey, V. Ramakantha, S.S. Chauhan, A.N.A. Kumar, *Wood is good: current trends and future prospects in wood utilization* (Springer, Singapore, 2017), p. 197.
[2] J. Wang, L. Wang, D.J. Gardner, S.M. Shaler, Z. Cai, Cellulose, **28**, 4511 (2021). DOI: 10.1007/s10570-021-03771-4
[3] J.Y. Zhu, U.P. Agarwal, P.N. Ciesielski, M.E. Himmel, R. Gao, Y. Deng, M. Morits, M. Österberg, Biotechnol Biofuels, **14**, 114 (2021). DOI: 10.1186/s13068-021-01963-5
[4] *Wood handbook: wood as an engineering material*, general technical report FPL-GTR-282 (U.S. Department of Agriculture Forest Service, Forest Products Laboratory, Madison, WI, USA, 2021). https://www.fs.usda.gov/treesearch/pubs/62200
[5] F. Jong, P. Clancy, Fire Mater., **28**, 209 (2004). DOI: 10.1002/fam.859
[6] A. Rindler, C. Hansmann, J. Konnerth, Wood Sci. Technol., **53**, 729 (2019). DOI: 0.1007/s00226-019-01100-4
[7] D. Tong, S.A. Brown, D. Corr, G. Cusatis, Holzforschung, **74**, 1011 (2020). DOI: 10.1515/hf-2019-0268

[8] H. Peng, L. Salmén, J. Jiang, J. Lu, Wood Sci. Technol., **54**, 1497 (2020). DOI: 10.1007/S00226-020-01221-1
[9] T.Y. Hsieh, F.C. Chang, Holzforschung, **72**, 1071 (2018). DOI: 10.1515/hf-2018-0056
[10] D.G. Hunt, Wood Sci. Technol., **38**, 479 (2004). DOI: 10.1007/s00226-004-0244-6
[11] T. Yu, A. Khaloian, J.-W. van de Kuilen, Eng. Struct., **259**, 114116 (2022). DOI: 10.1016/j.engstruct.2022.114116
[12] Yu.I. Golovin, Zavod. Lab., Diagn. Mater., **75** (1), 45 (2009) (in Russian). http://old-zldm.ru/upload/iblock/019/2009-1-45-59
[13] A.C. Fischer-Cripps, *Nanoindentation* (Springer, N.Y., 2011). DOI: 10.1007/978-1-4419-9872-9
[14] *Handbook of nanoindentation with biological applications*, ed. by M.L. Oyen (Pan Stanford Publ., 2011). DOI: 10.1201/9780429111556
[15] Yu.I. Golovin, *Nanoindentirovanie i ego vozmozhnosti* (Mashinostroenie, M., 2009) (in Russian).
[16] Yu.I. Golovin, Phys. Solid State, **63** (1), 1 (2021). DOI: 10.1134/S1063783421010108.
[17] Yu.I. Golovin, Phys. Solid State, **50** (12), 2205 (2008). DOI: 10.1134/S1063783408120019.
[18] Yu.I. Golovin, A.I. Tyurin, D.Yu. Golovin, A.A. Samodurov, S.M. Matveev, M.A. Yunack, I.A. Vasyukova, O.V. Zakharova, V.V. Rodaev, A.A. Gusev, Materials, **15**, 632 (2022). DOI: 10.3390/ma15020632
[19] Yu.I. Golovin, A.I. Tyurin, A.A. Gusev, S.M. Matveev, D.Yu. Golovin, I.A. Vasyukova, Tech. Phys. Lett., **48** (2), 73 (2022). DOI: 10.21883/TPL.2022.02.52855.19040.
[20] Yu.I. Golovin, A.I. Tyurin, A.A. Gusev, S.M. Matveev, D.Yu. Golovin, A.A. Samodurov, I.A. Vasyukova, M.A. Yunak, E.A. Kolesnikov, O.V. Zakharova, Tech. Phys., **92** (4), 484 (2022). DOI: 10.21883/TP.2022.04.53605.297-21.